論文 / 著書情報
Article / Book Information

Title	Concept of prismatic high temperature gas-cooled reactor with SiC coating on graphite structures
Author	Piyatida Trinuruk, Toru OBARA
Journal/Book name	Annals of Nuclear Energy, Vol. 63, , pp. 437-445
Issue date	2013, 9
URL	http://www.journals.elsevier.com/annals-of-nuclear-energy
DOI	http://dx.doi.org/10.1016/j.anucene.2013.08.019
Note	このファイルは著者（最終）版です。 This file is author (final) version.

Concept of prismatic high temperature gas-cooled reactor with SiC coating on graphite structures

Piyatida Trinuruk [a, *], Toru Obara [b]

[a] *Department of Nuclear Engineering, Tokyo Institute of Technology, 2-12-1-N1-19 Ookayama, Meguro-ku, Tokyo 152-8550, Japan*

[b] *Research Laboratory for Nuclear Reactors, Tokyo Institute of Technology,2-12-1-N1-19 Ookayama, Meguro-ku, Tokyo 152-8550, Japan*

Abstract

A 100-MW_{th} prismatic high temperature gas-cooled reactor was designed to be a long-life small reactor. To acquire a passive safety feature, the reactor was mainly improved with regard to graphite oxidation resistance. The concept of applying a silicon carbide coating layer on the surface of the graphite structures in the core was proposed to overcome any serious problem from graphite oxidation during unforeseen situations. However, there was concern that the deviation of neutronic and thermal properties of silicon carbide from graphite could affect the reactor operation and the heat transfer characteristics. Therefore, in this study we investigated the effects of applying a silicon carbide coating layer over the graphite structures from the neutronic and thermal-hydraulic points of view. Silicon carbide coating can lower the effective multiplication factor and shorten the reactor operating cycle, but not significantly. From the viewpoint of thermal-hydraulic operation, silicon carbide has lower thermal conductivity than that of graphite, so the layer of silicon carbide could act as a wall to keep the heat from moving across the layer. Under normal operation, the layer of silicon carbide coating had a less significant impact on the maximum fuel temperature, and the temperature remained lower than

* Corresponding author: Tel./Fax. +81 3 5734 2380
E-mail addresses: trinuruk.p.aa@m.titech.ac.jp (P. Trinuruk), tobara@nr.titech.ac.jp (T. Obara)

the maximum acceptable fuel temperature of 1495^{o}C for normal operation even when a thick layer of silicon carbide was applied. The silicon carbide later did have a significant impact on the increase of graphite moderating temperature. In summary, the reactor with a silicon carbide coating layer could safely operate under normal operating condition. Although the coating caused a decrease in the discharge burnup of the reactor, the improved passive safety of the reactor compensated for that disadvantage.

Keywords: Burnup calculation; Graphite oxidation; Passive safety; Prismatic high temperature gas-cooled reactor; Silicon carbide coating

1. Introduction

Since the accident at Fukushima Daiichi Nuclear Power Plant caused by the earthquake and tsunami in March 2011, the design concepts of nuclear power plants and reactors have been reconsidered, with more attention paid to nuclear safety and design issues. Innovative nuclear reactor designs such as high temperature gas-cooled reactors (HTGR) can achieve greater economic efficiency, reliability and inherent safety because of the distinguishing characteristics of the reactor design itself, which uses a graphite-moderated, helium-cooled, TRIstructural-ISOtropic (TRISO)-coated fuel particle coupled with a low power density design. Graphite is chemically inert and has large heat capacity, high strength, and oxidation stability, which provides a safety margin for the reactor core integrity during decay heat generation, whether by accidental pressurization or depressurization. Helium is an inert and single-phase coolant under all conditions, and a high outlet temperature can be achieved for high energy efficiency in electricity generation or hydrogen production.

Although graphite has advantageous properties for use in reactor cores, its mechanical and thermal properties can easily be degraded by oxidization, especially in accidents, which

might expose it to a high oxidation environment and high temperature. Among various gases in air ingress accidents, the most important oxidation reaction has been caused by oxygen gas (Choi et al., 2011). The effect of graphite oxidation can demolish the reactor core or impair the integrity of coated fuel particles, causing a release of radioactive material and fission products. In addition, the reaction between graphite and oxygen and/or water under unforeseen situations can occur in three kinds of reaction regime, that is, a chemical regime, a mass transfer regime and an in-pore diffusion-controlled regime, depending on the temperature. At low temperature, the reactant can penetrate the graphite, reducing its strength without changing its apparent geometries. At high temperature, surface oxidation can cause a loss of graphite mass (Iyoku et al., 1991).

To combat fragility at the surface caused by graphite oxidation, improved oxidation resistance was introduced by material coating. Silicon carbide (SiC) was a prospective coating material due to its capability to enhance mechanical strength, resist corrosion in aggressive environments, resist thermal shock, and retain all fission products within coated particle when implemented in TRISO fuel particles as a coating layer (Lamom, 2012). So far, the advantages of SiC coating have been examined only on the small scale, such as TRISO-coated particles. Our goal was to examine the use of SiC coating on the major parts of HTGR, such as graphite fuel blocks, graphite control rod blocks, and graphite fuel sleeves, in order to increase the safety margin of the reactor. Even though the layer of SiC on graphite material is very thin, the coating layer is expected having an impact on the nuclear reactor operation, especially on the criticality and the burnup characteristics, due to the poor neutronic properties of silicon. Similarly, the different thermal and mechanical properties of SiC can have an impact on the heat transfer characteristics in the reactor system.

The purpose of this study was to present a HTGR concept with SiC coating on the graphite structure and to investigate the impact of a SiC coating layer on the neutronic and thermal-hydraulic properties of the HTGR. In this study, the design criterion of the HTGR from the thermal-hydraulics point of view was based on the maximum acceptable fuel temperature at which the integrity of the coated fuel particle can be maintained under steady state normal operation.

2. Design concept of the reactor

2.1 Description of the reactor

A small prismatic HTGR was designed based on the specifications of a High Temperature Engineering Test Reactor (HTTR) (Nojiri et al., 1998). The rated thermal power was designed at 100 MW_{th}, with an average power density of 5.6 MW/m^3. Helium coolant flowed downward, with designed inlet and outlet coolant temperatures of 395^oC and 850^oC, respectively. The active core region consisted of 54 fuel blocks and 7 control rod blocks, surrounding with reflector region including 12 control rod blocks and 18 replaceable reflector blocks. Each column was contained 5 blocks, as shown in **Figure 1**. The detailed specifications of the reactor are given in **Table 1**. Thirty-three rods of 20 wt% enriched uranium used as nuclear fuel were inserted and uniformly distributed in each fuel block, and 3 holes were reserved for burnable poison rods to suppress the reactivity during operation. Low enriched uranium fuel of 20 wt% of ^{235}U was implemented to obtain the concept of a small reactor without on-site refueling.

In the safety requirements of HTGR, the maximum fuel temperature was determined based on the criterion that the coating layer of fuel particles must remain on the particles and retain fission products within the particles. The maximum fuel temperature should be under an

acceptable level at 1,495^{o}C during normal operation and not exceed 1,600^{o}C during any anticipated accident (Maruyama et al., 1994; Takada et al., 2004).

2.2 Coating with a SiC layer

SiC was selected as a coating barrier to protect graphite from oxidation. Generally, the SiC layer can be prepared to use on a graphite surface by a conventional technique called Chemical Vapor Deposition (CVD), which can detect a clear interface between the coating layer and the graphite material. Due to the difference in the thermal expansion coefficients between 4.7×10^{-6} K^{-1} of SiC and 4.06×10^{-6} K^{-1} of graphite, therefore, thermal stress can take place and induce instability of the coating layer, resulting in splitting and cracking between the coating and the substrate (Fujii et al., 1992, 1993; Zhu et al., 1999).

An advanced material called Functionally Graded Material (FGM) or compositionally gradient material was developed to minimize thermal stress on the coating interface. The graphite was first coated with SiC, and then SiC was gradually dispersed in the microstructure of graphite (SiC/C) by the reaction of gaseous silicon monoxide (SiO), causing the clear interface to vanish (Fujii et al., 1992, 1993).

Double-coating with a layer of CVD and FGM SiC/C exhibited a greater potential for oxidation protection of graphite than that offered by a single coating layer of either CVD SiC or FGM SiC/C. Even though the coating layer of FGM SiC/C only cannot perform well to reduce the oxidation rate when considering the change of mass, it can maintain the shape of the sample by the stability of the coating layer itself (Fujii et al., 1992, 1993).

From the viewpoint of mechanical properties, a SiC layer applied with the CVD technique on either a graphite substrate or on FGM SiC/C graded material can improve the

bending strength approximately twofold compared to that of bare graphite, while the FGM SiC/C grade layer did not have this effect. However, SiC coating by either technique can remarkably improve the hardness of the material (Nakano et al., 1997).

To simplify the model calculation, we assumed that the graphite structure was coated with a SiC layer by the CVD technique, because this method can provide a clear interface indicating the coating layer thickness. The overall dimensions of the components in the reactor after coating with a SiC layer were controlled by removing the graphite surface and replacing it with an identical amount of SiC coating layer on top of the remaining graphite. The SiC coating was concentrated on the outer surface of the graphite blocks, including the fuel blocks, control rod blocks and reflector blocks, the inner surface of the coolant channels and the outer surface of the graphite fuel sleeves. The minimum thickness of the SiC coating layer that would be effective for oxidation protection was identified as 100 μm in a previous study (Fujii et al., 1992, 1993). In the present study, we varied the thickness of the SiC coating layer between 100, 200, 500 and 700 μm, respectively. The effect of thermal stress due to the difference in the thermal expansion coefficients of two different materials was ignored in this study.

3. Neutronic analysis

3.1 Methodology of neutronic analysis

The main purpose of neutronic analysis was to observe the effect of a SiC coating on the burnup characteristics. Continuous energy Monte Carlo code MVP and MVP-BURN, developed by JAERI (Nagaya et al., 2005), were used to evaluate the burnup characteristics of the whole-core geometry. The burnup analysis was performed with a uniform temperature of 800 K for the coolant, fuel sleeve, moderator and fuel by using JENDL-4.0 cross section data library. We

ignored the insertion of burnable poison in the operation so we could observe the effect of the SiC coating only. The fuel packing fraction was designed to be 30%. The statistical geometry model (STGM), which was implemented in MVP and MVP-BURN, was applied to analyze the double heterogeneity effect of the coated fuel particles in the graphite matrix. The statistical errors of the effective multiplication factor (k_{eff}) for all burnup calculations were controlled within 0.05%, which was obtained on 140 batches including 20 skip batches with 15,000 neutron histories in a batch.

3.2 Impact of SiC coating on core performance

The concept of SiC coating on the graphite surface was proposed to increase the safety margin in terms of oxidation prevention. **Figure 2** illustrates the burnup characteristic of five different HTGR designs: conventional HTGR and the HTGRs with 100, 200, 500, and 700 μm of SiC coating layer, respectively. The result of burnup calculation indicated that the k_{eff} was slightly reduced and relatively more decreased when the thickness of the SiC layer increased. The core without burnable poison induced extremely high excess reactivity at the beginning of the reactor cycle (BOC) because of initial fresh fuel loading, as summarized in **Table 2**. When the constraint of the k_{eff} was determined at 1.00, the reactivity in the first burnup stage was extremely high at more than 30% Δk/k. This is because a large amount of excess thermal neutrons were captured by fissile isotopes ^{235}U and contributed to a fission reaction.

As designed, a 100-MW_{th} HTGR without SiC coating can achieve high discharge burnup at 104.5 GMd/t and sustain the reactor operation period up to 1,670 EFPDs (effective full power days) when 20 wt% ^{235}U is used as the nuclear fuel. In a comparison between with and without a SiC coating layer, we found that a thick SiC-coated layer such 700 μm shortened the discharge

burnup from 104.5 GWd/t to 96.2 GWd/t and reduced the reactor operation period from 1,670 EFPDs to 1,536 EFPDs. The decreased k_{eff} resulted from the replacement of graphite with SiC in the reactor. Because silicon has a lower scattering cross section and larger capture cross section as compared to graphite, which is itself a poor moderator, the SiC layer can make the neutron spectrum harden slightly.

Figure 3 shows the change of the neutron spectrums in the fuel particles. The neutron spectrum was slightly harder with increased thickness of the SiC coating layer as a result of lower moderating material. Next, we analyzed the impact of the hard spectrum on the transmutation by notice the change of nuclide number densities of the main isotopes. **Table 3** shows the change of nuclide number densities of ^{235}U, ^{238}U, ^{239}Pu and ^{241}Pu for the whole-core on the 1,600th day of reactor operation compared to the beginning of reactor operation. The results show that nuclide number densities of fissile isotopes ^{239}Pu and ^{241}Pu increased slightly when the SiC coating layer was applied and increased relatively more when the thickness of the SiC layer increased. The harder neutron spectrum in the HTGR caused by coupling with a SiC coating layer enhanced the capability of fertile material ^{238}U to capture a neutron and easily convert to fissile isotope ^{239}Pu by a process of transmutation. However, we notice that such a small amount of SiC coating cannot effectively increase the transmutation of fertile nuclide ^{238}U to fissile nuclides ^{239}Pu and ^{241}Pu, as we expected.

3.3 Impact of SiC coating on reactor power

In this design, 20 wt% enriched uranium was arranged uniformly throughout the core, so the peak power density could occur at the center of the core, which was undesirable and uneconomical. **Figure 4** shows the average power density distribution of the whole core in the axial direction for five different HTGR designs. We can note that the average power density

throughout the core was 5.6 MW/m^3. The maximum power density of all reactors took place at the middle of the core with the maximum value of about 6.79 - 6.88 MW/m^3, depending on the reactor design. With SiC coating on the graphite, the power density was slightly higher than that of a reactor without SiC coating only at the core center, but it was slightly lower at the other positions in the core, especially when it was close to the reflector region. However, when considering the whole core, the space integration of each power density curve was equal for all reactors. Theoretically, the hard spectrum in the thermal reactor could cause a decreased fission reaction rate of ^{235}U due to a smaller capture cross section of ^{235}U. By this effect, the power density in a reactor with a SiC coating could decrease and be smaller than that of a reactor without SiC coating, but the results were different. The SiC layer which coated on the outer surface of the reflector block exhibited as a poor reflecting material due to the lower amount of graphite which increased the neutron leakage or the neutron migration. This resulted in the reduction of thermal neutron flux in the fuel zone, which is close to the reflector region, and a shift of thermal neutron flux at the core center.

In this study, our objective from the viewpoint of thermal-hydraulic analysis was to evaluate the occurrence of the maximum fuel temperature by using the conservative value of the maximum power density which took place on the fuel rods. When the reactor was designed with uniform fuel distribution, the maximum power density of a fuel rod appeared at the center of the core, and this value was used as the power generation in the analysis. This design condition could provide a greater safety margin in terms of the designed fuel temperature.

Figure 5 shows the axial power density profiles of the fuel rods at the peak power position during the BOC. The reactor power of uniform fuel distribution in the axial direction can be described by the cosine function. The maximum power density at the peak position was around 9.5 MW/m^3. We note that the power density in the reactor with SiC coating increased

slightly and was distinctly noticeable at the core center. However, the total power throughout the fuel rod for all reactors was the same.

The power peaking factor (PPF) is defined as the ratio of maximum local power density to average power density at burnup, as follows:

$$\mathrm{PPF} = \frac{\text{Maximum local power density}}{\text{Average power density}} \quad (1)$$

The maximum PPF was approximately 1.65, with the statistical error less than 0.15% for all cases, and it occurred at the first stage of reactor operation by the high reaction rate of fissile materials at the center and then gradually decreased during the burnout of fissile materials, as shown in **Figure 6**. Adding the SiC coating layer had a small effect on the PPF that was difficult to observe. **Figure 7** shows the history of power density distribution in the radial direction of 5 fuel block layers during the burnup periods of 0, 320, 639, 958 and 1,437 EFPDs for the conventional reactor and that of coupling with a 200-μm SiC coating layer. For both reactors, the power density distributions at the BOC peaked at the center and were greatly scattered for each layer. Then, the peak of power density decreased, becoming closer in each layer during the middle of the reactor cycle (MOC) and flattening at the end of the reactor cycle (EOC).

4. Thermal-hydraulic analysis

4.1 Methodology of thermal-hydraulic analysis

Thermal-hydraulic analysis was carried out for a single sub-channel via finite element software named COMSOL Multiphysics 4.2a (COMSOL AB, 2011). The model geometry was developed with 2-dimensional axisymmetry with r-z coordinates that consisted of the fuel compact, gap, graphite sleeve, cooling channel, graphite moderator and coating of SiC layer on the graphite surface. The hexagonal lattice of the graphite moderator was simplified to be

equivalent to a cylinder, as shown in **Figure 8**, and **Figure 9** shows the model geometry of sub-channel analysis for the whole length of the reactor.

Helium coolant flowed vertically downward through the cooling channel and was assumed to be uniformly distributed throughout the cooling channel. Therefore, the mass flow through a single sub-channel can be estimated, if the total cross section of the cooling channels is known. The coolant flow rate and its temperature at inlet were determined as inlet boundary conditions, while the pressure outlet was specified as an outlet boundary condition. To establish a conservative boundary condition, the outer boundary of the model geometry was specified with the adiabatic boundary condition, that is, with no heat crossing the boundary. **Table 4** shows the operating conditions of the 100-MW_{th} HTGR.

In thermal-hydraulic analysis, the power distribution of the fuel rod in the axial direction was analyzed by the Monte Carlo code MVP-BURN. The power generation from the fuel rod at the center of the core can be calculated from the production of the power density in the fuel particles and the volume of the fuel pin. These values represented conservative power generation for this analysis under the assumption that the power generation was conducted from the fuel pin only. The other sources of power generation such as in the moderator and in the reactor structure by the gamma heating effect were ignored in this study.

We used IG-110, a fine-grained isotropic graphite, as the graphite material in the core component, as it is widely used in HTGR due to its unique characteristics. The thermal properties of IG-110 and SiC were taken into account as a function of temperature and irradiation. Wu et al. (1994) had reported the effect of neutron irradiation as a function of irradiation dose and the temperature, which degrade the materials. The degradation of the material properties was not just the result of thermal-hydraulic behaviors; it also was primarily

caused by an increased resistance to photon heat transport, resulting in an accumulation of fission products in the lattice and radiation damage.

4.2 Parametric survey on thermal-hydraulic analysis of the reactor

A parametric survey was performed the analysis on one fuel block of a single sub-channel. The goal of this survey was to reveal the effect of the reactor operating condition on the heat transfer characteristic, and thus the variation of the pressure outlet and the inlet velocity of the coolant were determined. The power distribution in a fuel rod at the center of the reactor core without a SiC coating layer was represented as the power generation from a fuel rod in this analysis. The power was assumed to be constant throughout the fuel rod and equal for all cases so we could determine the particular effect of SiC coating. **Table 5** shows the calculation results of the maximum fuel temperature, the average temperature of coolant outlet, the maximum temperature at the outermost part of the cell, and the pressure drop when the SiC coating layer thickness and the coolant flow conditions were varied. Under energy conservation at a steady state condition, if the heat generation in the calculation model were set up with the same values for the case of 0, 100, 200, 300, 400 and 500 μm, then the average outlet coolant temperature should be equal under the same coolant flow condition and differ if the coolant flow condition changes. The results in **Table 5** show that the average outlet coolant temperatures under the same coolant conditions but different thicknesses of SiC coating layer were not exactly the same. This deviation was caused by the difference of geometry meshing. However, the standard deviation for all conditions was within 4.8^{o}C for the outlet coolant temperature, 2.2^{o}C for the maximum fuel temperature and 3.7^{o}C for the maximum temperature at the outer surface of cell. Therefore, the error in the calculation results can be accepted under the deviation of 4.8^{o}C based on the result of the average outlet coolant temperature. Hence, we conclude that varying the SiC layer

thickness did not have a significant impact on the change of maximum fuel temperature because the standard deviation of maximum fuel temperature results was lower than that of outlet coolant temperature.

In addition, the results show that the change of temperature was mainly caused by the change of cooling operating conditions such as the coolant flow rate and its pressure. The variation of SiC layer thickness did not have a significant impact on the change of maximum fuel temperature.

4.3 Thermal-hydraulic analysis along the whole length of the core

Next, we performed a thermal-hydraulic analysis under the boundary condition of 5.0 MPa as the pressure outlet and 5.0 m/s as the coolant inlet velocity. The model geometry was developed on a single sub-channel of the whole length of the reactor core, including 2 top reflector blocks, 5 fuel blocks, and 2 bottom reflector blocks, as shown in **Figure 9**. The increase in number of fuel blocks plus with reflector blocks made the flow distance of the coolant longer which caused the pressure to drop by 22 – 38 kPa which were relatively high as compared to the pressure drop in one fuel block of 0.13 – 0.19 kPa. However, the results showed that the pressure drop did not exceed the limit of the reactor design at 50 kPa.

Under normal steady state condition and the assumption of equal power density distribution, the results of average coolant outlet temperature for all cases should be equal due to energy conversion, but the results in **Table 6** show that this was not the case. The deviation of outlet coolant temperature was caused by the difference in meshing of the model geometry, as mentioned above. The result shows that the reactor core without SiC coating induced the maximum fuel temperature up to 1,320^{o}C, and the temperature increased slightly with a SiC

layer of 500 μm or 700 μm. The deviation of those maximum fuel temperatures was less than the standard deviation of 3.6^{o}C, which was less than an acceptable value of the calculation error of 4.7^{o}C, as described above. Therefore, the addition of SiC coating under the same power distribution did not increase the fuel temperature further, and the maximum fuel temperature was less than that given in the HTGR design.

Otherwise, the SiC layer had the greatest effect on the temperature at the outermost surface of the graphite cell. Poor heat conductivity of the SiC layer acted as a barrier against the heat penetrating from the fuel rod through the graphite block region, which was why the temperature of the graphite surface in the reactor without SiC coating was higher than those of the cases with SiC coating, as illustrated in **Figure 10**. **Figure 11** shows the axial temperature distribution of the fuel and at the outermost surface of the graphite block. The temperature profiles of the fuel were indistinctively different from case to case, but the largest difference of the temperature was about 60^{o}C, occurring at the outermost surface of the graphite moderator.

From the viewpoint of the same power density analysis, little effect can be recognized by the change of the SiC layer thickness. Therefore, we did the next analysis by using the actual power generated in the fuel rod for the individual cases of SiC layer thickness, as shown in **Table 6**. As noted in Section 3.3, the addition of SiC coating to the reactor can cause a shift of the power density profile in the reactor due to the change of the thermal neutron flux profile. Compared to the reactor without a SiC coating layer, coating with a SiC layer caused a higher peak power at the middle of the core and a more gradual decrease in temperature, which caused a lower power density when the radius increased. A small increment of power generated in the fuel rod by a SiC coating layer caused the maximum fuel temperature change of about 20-26^{o}C.

However, the maximum fuel temperature of all cases existed under the temperature limit of the reactor design, 1,495^{o}C.

4.4 Effect of the variation of SiC thermal conductivity

In the preceding section, we mainly considered how the variation of SiC layer thickness affected the heat transfer characteristic, but another dominant factor influencing the heat transfer behavior, especially in terms of conduction heat transfer, was the thermal conductivity of the material itself. Therefore, another analysis was performed in which we varied the thermal conductivity of SiC and graphite, respectively. **Table 7** shows the effect of variation of graphite's thermal conductivity on the material temperature, and **Table 8** shows the effect of variation of SiC's thermal conductivity on the change of temperature. We found that better thermal conductivity of either SiC or graphite induced a good heat transfer process, which, in turn, caused the fuel temperature to become lower, and vice versa. Nevertheless, this factor had less impact on the change of coolant temperature and the temperature at the outermost surface of graphite.

5. Discussion

From the viewpoint of neutronic characteristics, a HTGR in which the graphite oxidation resistance was improved by coating with a SiC layer can be made to exhibit decreased reactivity by removing a small amount of moderating material and replacing it with the same amount of a poor moderating material such as SiC in the core. The thicker the SiC layer, the lower the reactivity. However, even a SiC layer with conservative thickness of 700 μm induced a lower discharge burnup of about 8 GWd/t for an entire burnup period and shortened the nuclear fuel

cycle about 130 days as compared with the reactor without SiC coating, though the outcome was worthwhile in terms of passive safety.

From a thermal-hydraulic point of view, SiC had lower thermal conductivity than graphite, and therefore, the SiC layer acted as a barrier to obstruct the heat transferred radially to adjacent material that also penetrated to the helium coolant. This effect can be clearly seen from the difference in temperature at the outermost surface of the cell between with and without the SiC layer. The impact of the SiC coating layer caused the biggest deviation of temperature at the outermost surface of the cell of about 60^{o}C. However, according to the past experience of licensing procedure, a temperature uncertainty of about 150^{o}C can be expected for the very high temperature reactor (VHTR) operating condition (Haque et al., 2006).

On the other hand, a change in the fuel temperature as an effect of SiC coating was hard to recognize. Under the same power generation, the SiC coating did not affect the fuel temperature. The impact of the SiC coating layer on the maximum fuel temperature did not exceed the limit condition of the HTGR design of 1,495^{o}C for normal reactor operation in any of the cases. The conservation value of fuel temperature was 1,347^{o}C, which was obtained in the case of a SiC layer of 700 μm with the actual power generation in the core. That result means that the reactor still had a safety margin of designed fuel temperature of about 148^{o}C. Based on the existing safety margin of the designed fuel temperature under normal operation, the HTGR with a SiC coating layer could be operated safely under the criteria of reactor design in the case of an accident.

6. Conclusions

A 100-MW_{th} prismatic HTGR of 20 wt% enriched uranium was designed. The concept of using a SiC coating layer on the graphite structure to improve the graphite oxidation resistance

was proposed as a passive safety feature of the HTGR. The effect of a coating layer of SiC was confirmed from the neutronic point of view and the thermal-hydraulic point of view; adding a small amount of SiC instead of graphite as a coating layer can have a small impact on the neutronic characteristic by slightly decreasing the reactivity and shortening the fuel burnup life cycle because of the large neutron absorption cross section of silicon in SiC. Regarding the heat transfer behavior, the fuel temperature was impacted very little by the coating of a SiC layer under the same power distribution, but a small increase in the fuel temperature took place when the actual power generated in the reactor core was taken into account.

We conclude that under normal operation, the effect of a SiC coating is acceptable from the viewpoint of the neutronic and heat transfer via the maximum fuel temperature, besides the proven performance with regard to the oxidation resistance and mechanical properties. The implementation of SiC coating is a practical and achievable passive safety feature.

7. References

Choi, W. K., Kim, B.J., Kim, E.S., Chi, S.H., Park, S.J., 2011. Oxidation Behavior of IG and NBG Nuclear Graphites. Nucl. Eng. and Des. 241, 82-87.

COMSOL AB, 2011. COMSOL Multiphysics User's Guide Version 4.2a.

Fujii, K., Imai, H., Nomura, S., Shindo, M., 1992. Functionally Gradient Material of Silicon Carbide and Carbon as Advanced Oxidation-resistant Graphite, J. Nucl. Mater. 187, 204-208.

Fujii, K., Nakano, J., Shindo, M., 1993. Improvement of the Oxidation Resistance of a Graphite Material by Compositionally Gradient SiC/C layer. J. Nucl. Mater. 203, 10-16.

Haque, H., Feltes, W., Brinkmann, G., 2006. Thermal Response of a Modular High Temperature Reactor during Passive Cooldown under Pressurized and Depressurized Conditions. Nucl. Eng. and Des. 236 (5-6), 475-484.

International Atomic Energy Agency, 2001. Design and Evaluation of Heat Utilization Systems for the High Temperature Engineering Test Reactor. IAEA-Tecdoc-1236. IAEA, Vienna, Austria.

Iyoku, T., Shiozawa, S., Ishihara, M., Arai, T., Oku, T., 1991. Graphite Core Structures and Their Structural Design Criteria in the HTTR. Nucl. Eng. and Des. 132, 23-30.

Lamom, J., 2012. Properties and Characteristics of SiC and SiC/C Composites, in: Konings, R.J.M., Comprehensive Nuclear Materials: Volume 3. Elsevier, Spain, pp. 323-338.

Maruyama, S., Fujimoto, N., Sudo, Y., Murakami,T., Fujii, S., 1994. Evaluation of Core Thermal and Hydraulic Characteristics of HTTR. Nucl. Eng. and Des. 152, 183-196.

Nagaya, Y., Okumura, K., Mori, T., Nakagawa, M., 2005. MVP/GMVP II: General Purpose Monte Carlo Codes for Neutron and Photon Transport Calculations Based on Continuous Energy and Multigroup Methods. JAERI 1348. Japan Atomic Energy Research Institute.

Nakano, J., Fujii, K., Yamada, R., 1997. Mechanical Properties of Oxidation-Resistant SiC/C Compositionally Graded Graphite Materials, J. Am. Ceram. Soc. 80 (11), 2897-2902.

Nojiri, N., Nakano, M., Ando, H., Fujimoto, N., Takeuchi, M., Fujisaki, S., Yamashita, K., 1998. Preliminary Analyses for HTTR's a Start-up Physics Tests by Monte Carlo Code MVP. JAERI-Tech 98-032.

Takada, E., Nakagawa, S., Fujimoto, N., Tochio, D., 2004. Core Thermal-hydraulic Design, Nucl. Eng. and Des. 233, 37-43.

Wu, C.H., Bonal, J.P., Kryger, B., 1994. The Effect of High-dose Neutron Irradiation on the Properties of Graphite and Silicon Carbide. J. Nucl. Mater. 208, 1-7.

Zhu, Q., Qiu, X., Ma, C., 1999. Oxidation Resistant SiC Coating for Graphite Material, Carbon. 37, 1475-1484.

Table captions

Table 1 Design specifications of 100-MW_{th} HTGR

Table 2 The neutronic analysis of 100-MW_{th} HTGR without burnable poison insertion

Table 3 The change of nuclide density of ^{235}U, ^{238}U, ^{239}Pu and ^{241}Pu for the whole reactor from the BOC to the 1600^{th} day of reactor operation ($ND_{1600}{}^{th}$ - ND_{BOC})

Table 4 Design operating conditions of 100-MW_{th} HTGR

Table 5 Parametric survey on the effect of SiC layer thickness and the environmental conditions for one fuel block when the insertion of burnable poison is negligible

Table 6 Thermal-hydraulic analysis for the whole length of the core

Table 7 Thermal-hydraulic analysis for the whole length of the core at various levels of thermal conductivity of graphite

Table 8 Thermal-hydraulic analysis for the whole length of the core at various levels of thermal conductivity of SiC

Table 1 Design specification of 100-MW_{th} HTGR

Core parameter	
Thermal power (MW_{th})	100
Equivalent core radius (m)	2.8
Effective core height (m)	2.9
Average power density (MW/m^3)	5.7
Number of fuel blocks (blocks)	270
Number of fuel columns (columns)	54
Number of fuel pin in a block	33
Fuel	
Fuel	UO_2 in TRISO particle
Uranium enrichment	20.0 wt%
Packing fraction (%)	30
Coating material	PyC / PyC / SiC / PyC
Thickness (μm)	0.061 / 0.0306 / 0.02875 / 0.0459
Density (g/cm^3)	1.10 / 1.85 / 3.20 / 1.85
Graphite block	
Material	Graphite IG-110
Density (g/cm^3)	1.77
Graphite matrix (fuel compact)	
Material	Graphite IG-110
Density (g/cm^3)	1.7
Fuel sleeve	
Material	Graphite IG-110
Density (g/cm^3)	1.75
Replaceable reflector	
Material	Graphite IG-110
Density (g/cm^3)	1.75
Fixed reflector	
Material	PGX graphite
Density (g/cm^3)	1.73
SiC coating layer	
Material	SiC
Density (g/cm^3)	3.20

Table 2 The neutronic analysis of 100-MW_{th} HTGR without burnable poison insertion

SiC coating	Initial k_{eff}	$\rho^{*,**}$ (%Δk/k)	Discharge burnup** (GWd/t)	EFPDs** (days)
No SiC	1.474 ± 0.00052	32.16	~104.5	1,670
100 μm	1.470 ± 0.00058	31.96	~103.2	1,645
200 μm	1.463 ± 0.00051	31.65	~102.2	1,630
500 μm	1.448 ± 0.00054	30.94	~98.5	1,572
700 μm	1.437 ± 0.00055	30.43	~96.2	1,536

Notes: * Initial excess reactivity, ** Determined the constraint of k_{eff} at 1.00

Table 3 The change of nuclide density of ^{235}U, ^{238}U, ^{239}Pu and ^{241}Pu for the whole reactor from the BOC to the 1600th day of reactor operation ($ND_{1600^{th}} - ND_{BOC}$)

Case	$k_{eff,\ at\ 1600^{th}}$	Nuclide density of main isotope (atom/b.cm)			
		^{235}U	^{238}U	^{239}Pu	^{241}Pu
No SiC	1.017 ± 0.00046	-1.0802E-01	-3.1314E-02	8.1322E-03	2.4177E-03
SiC 100 μm	1.012 ± 0.00043	-1.0787E-01	-3.1472E-02	8.2121E-03	2.4245E-03
SiC 200 μm	1.008 ± 0.00047	-1.0779E-01	-3.1578E-02	8.2461E-03	2.4439E-03
SiC 500 μm	0.994 ± 0.00044	-1.0790E-01	-3.2240E-02	8.4393E-03	2.5106E-03
SiC 700 μm	1.004 ± 0.00043	-1.0775E-01	-3.2431E-02	8.6185E-03	2.5716E-03

Table 4 Design operating conditions of 100-MW_{th} HTGR

Parameter	Value	Unit
Coolant	Helium	
Coolant temperature inlet / outlet	395 / 850	^{o}C
Mass flow rate	42.3	kg/s
Outlet pressure	5.0	MPa
Pressure dropped	< 50	kPa
	Based on GM-HTR (IAEA, 2001)	

Table 5 Parametric survey on the effect of a SiC layer thickness and the environmental conditions for one fuel block when the insertion of burnable poison is negligible

SiC layer thickness	Maximum fuel temp. (°C)			Average outlet coolant temp. (°C)			Maximum temp. at outer surface of cell (°C)			Pressure drop (kPa)
	(a)	(b)	(c)	(a)	(b)	(c)	(a)	(b)	(c)	(a) – (c)
0 μm	1,601	1,584	1,575	897	858	838	668	638	623	0.17 – 0.22
100 μm	1,602	1,584	1,575	902	864	844	670	640	624	0.13 – 0.16
200 μm	1,603	1,585	1,575	905	868	849	673	645	630	0.14 - 0.18
300 μm	1,604	1,588	1,579	902	865	848	670	640	628	0.14 – 0.17
400 μm	1,605	1,588	1,579	904	867	848	671	643	628	0.15 – 0.19
500 μm	1,605	1,588	1,579	908	871	852	676	648	633	0.14 – 0.18
Standard deviation	1.6	2.0	2.2	3.7	4.4	4.8	2.8	3.7	3.7	

Notes: (a) V_{in} 2.5 m/s and P_{out} 4.0 MPa,
(b) V_{in} 2.5 m/s and P_{out} 5.0 MPa, and
(c) V_{in} 3.5 m/s and P_{out} 4.0 MPa

Table 6 Thermal-hydraulic analysis for the whole length of the core

SiC thickness (μm)		**0***	**500***	**700***	**500**	**700**
Power generated in fuel rods (MW/m^3)	Block 1		49.2		48.1	49.4
	Block 2		66.4		67.8	68.9
	Block 3		73.8		75.4	75.9
	Block 4		66.9		69.0	67.3
	Block 5		49.0		47.9	44.9
Max. fuel temp. (^oC)		1,320	1,325	1,327	1,340	1,346
Avg. coolant outlet temp. (^oC)		818	821	812	823	814
Max. temp. at outer surface of the cell (^oC)		866	799	803	784	806
Pressure drop (kPa)		38	22	22	22	22

Note: * The calculation was based on the same power distribution as that obtained in the case of a reactor without SiC coating.

Table 7 Thermal-hydraulic analysis for the whole length of the core at various levels of thermal conductivity of graphite

	Maximum fuel temperature (^{o}C)			Max. temp. at outer cell surface (^{o}C)		
SiC coating	0 μm	500 μm	700 μm	0 μm	500 μm	700 μm
k_{gp} (T) (Ref.)	1,320	1,325	1,327	866	799	803
k_{gp} = 15 W/m. ^{o}C	1,320	1,325	1,326	866	799	804
k_{gp} = 20 W/m. ^{o}C	1,299	1,306	1,309	865	799	803
k_{gp} = 25 W/m. ^{o}C	1,287	1,295	1,299	865	794	802

Table 8 Thermal-hydraulic analysis for the whole length of the core at various levels of thermal conductivity of SiC

	Maximum fuel temperature (^{o}C)			Max. temp. at outer cell surface (^{o}C)		
SiC coating	0 μm	500 μm	700 μm	0 μm	500 μm	700 μm
k_{SiC} = 10 W/m.^{o}C	-	1,328	1,331	-	799	803
k_{SiC} = 12.8 W/m.^{o}C (Ref.)	-	1,325	1,327	-	799	803
k_{SiC} = 15 W/m.^{o}C	-	1,324	1,325	-	794	803

Figure captions

Figure 1 Core arrangement, fuel block and control rod block of a 100-MW_{th} HTGR

Figure 2 Burnup characteristics of a 100-MW_{th} HTGR without the insertion of burnable poison

Figure 3 Distribution of the neutron spectrum in fuel particles compared between the reactor without a SiC coating layer and with a SiC coating layer of 500 μm during the beginning of the reactor cycle.

Figure 4 The average axial power density distribution of the whole core during the beginning of the reactor cycle

Figure 5 The axial power density distribution on the fuel rods at the peak power position during the beginning of the reactor cycle

Figure 6 Power peaking factor of an HTGR during core life

Figure 7 History of the radial power density distribution for 5-fuel block layers at the reactor operation of 0, 320, 639, 958 and 1,437 EFPDs for a conventional reactor and a reactor with a SiC coating layer of 200 μm coupled with no insertion of burnable poison

Figure 8 Cross-section view of single sub-channel model geometry

Figure 9 Geometry of sub-channel analysis for the whole length of the reactor

Figure 10 The temperature distribution in the radial direction at the middle of the core

Figure 11 The temperature distribution in the axial direction

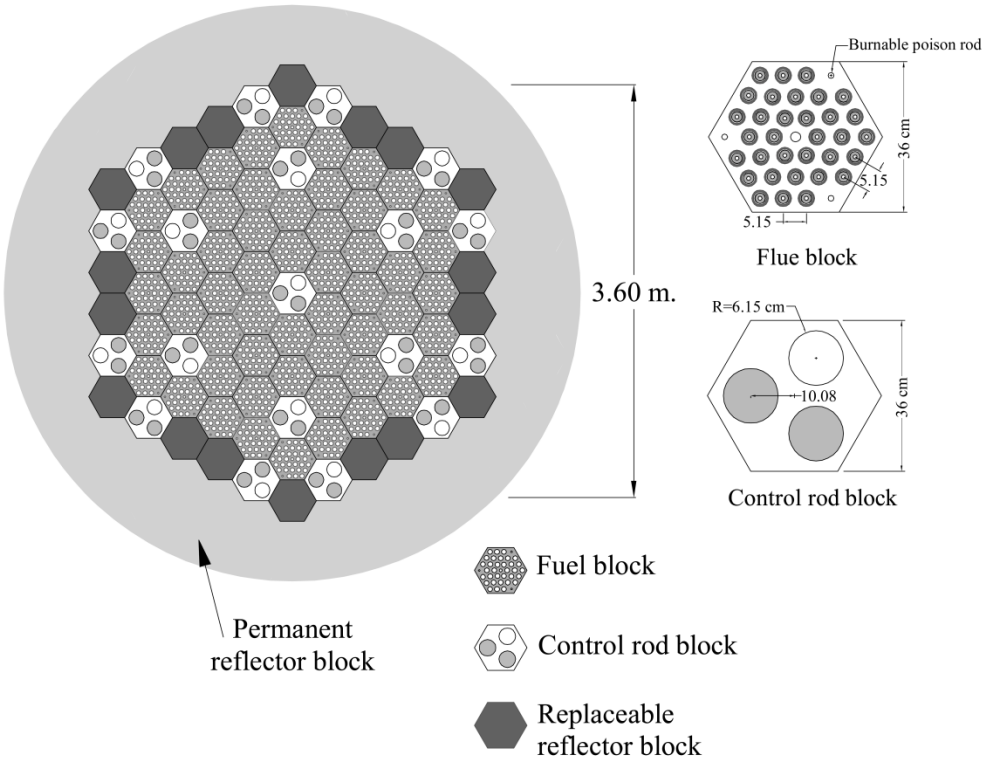

Figure 1 Core arrangement, fuel block and control rod block of a 100-MW_{th} HTGR

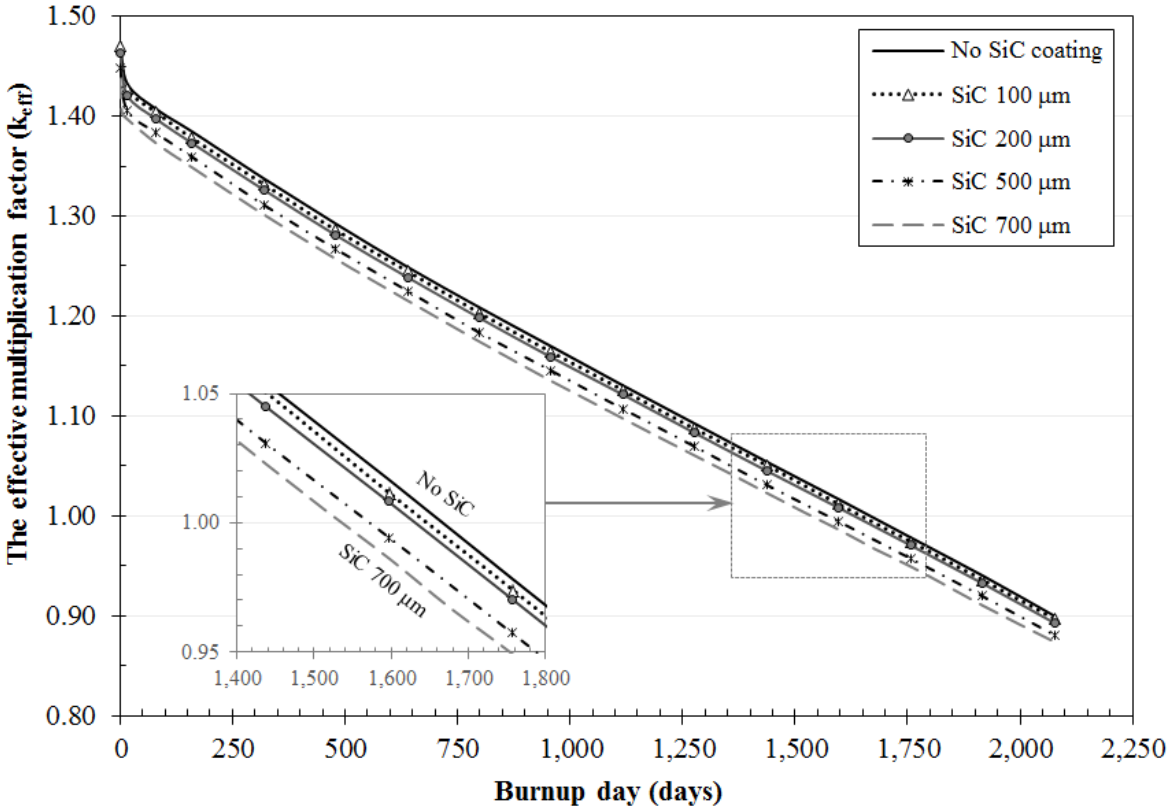

Figure 2 Burnup characteristics of a 100-MW_{th} HTGR without the insertion of burnable poison

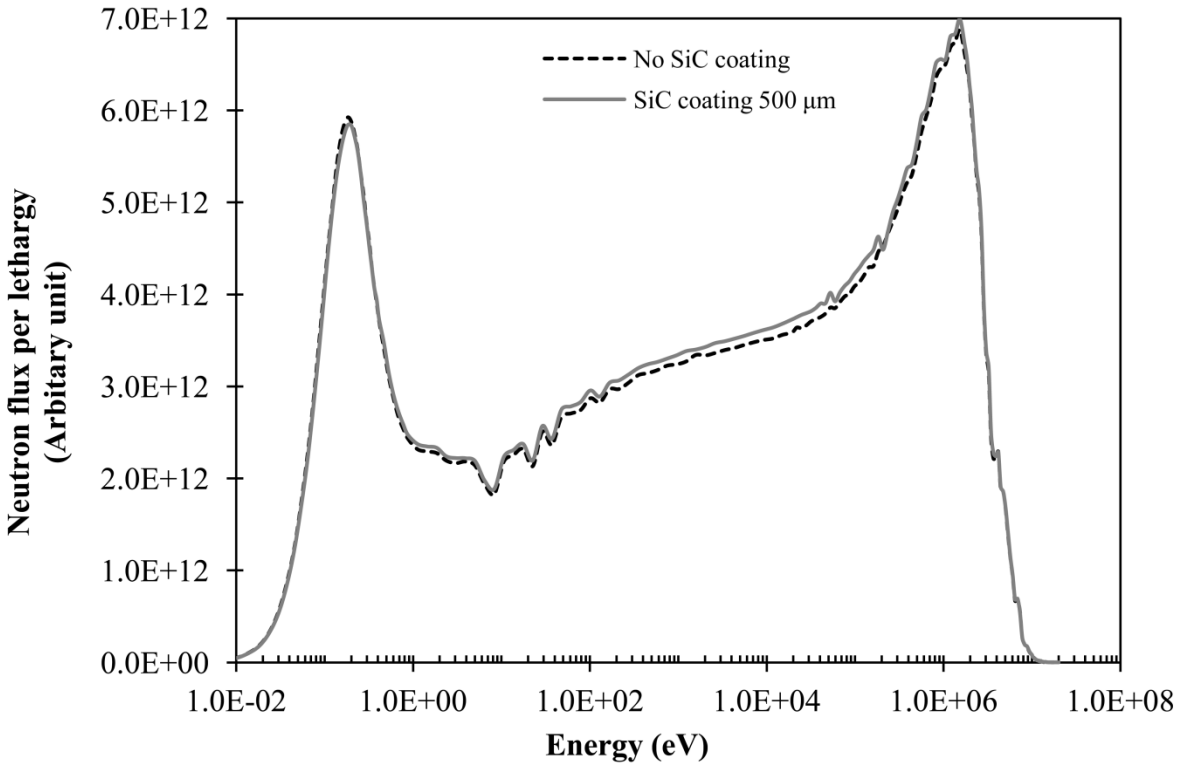

Figure 3 Distribution of the neutron spectrum in fuel particles compared between the reactor without a SiC coating layer and with a SiC coating layer of 500 μm during the beginning of the reactor cycle

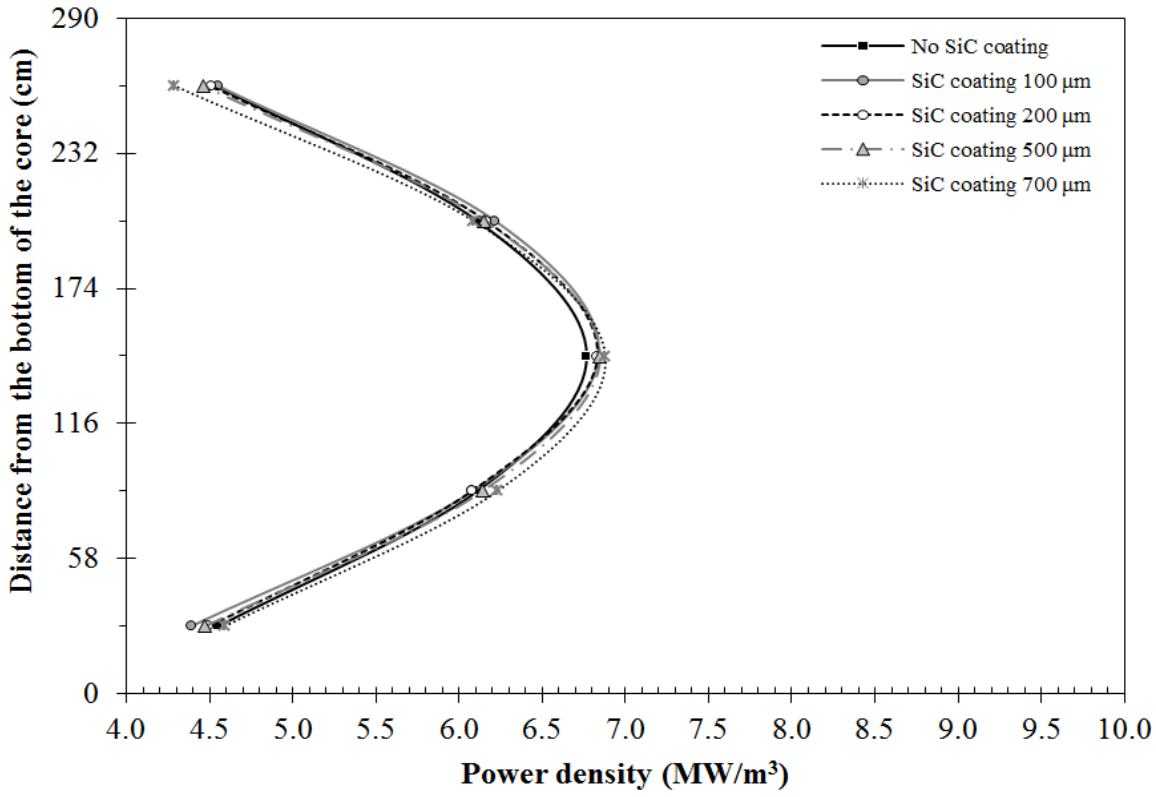

Figure 4 The average axial power density distribution of the whole core during the beginning of the reactor cycle

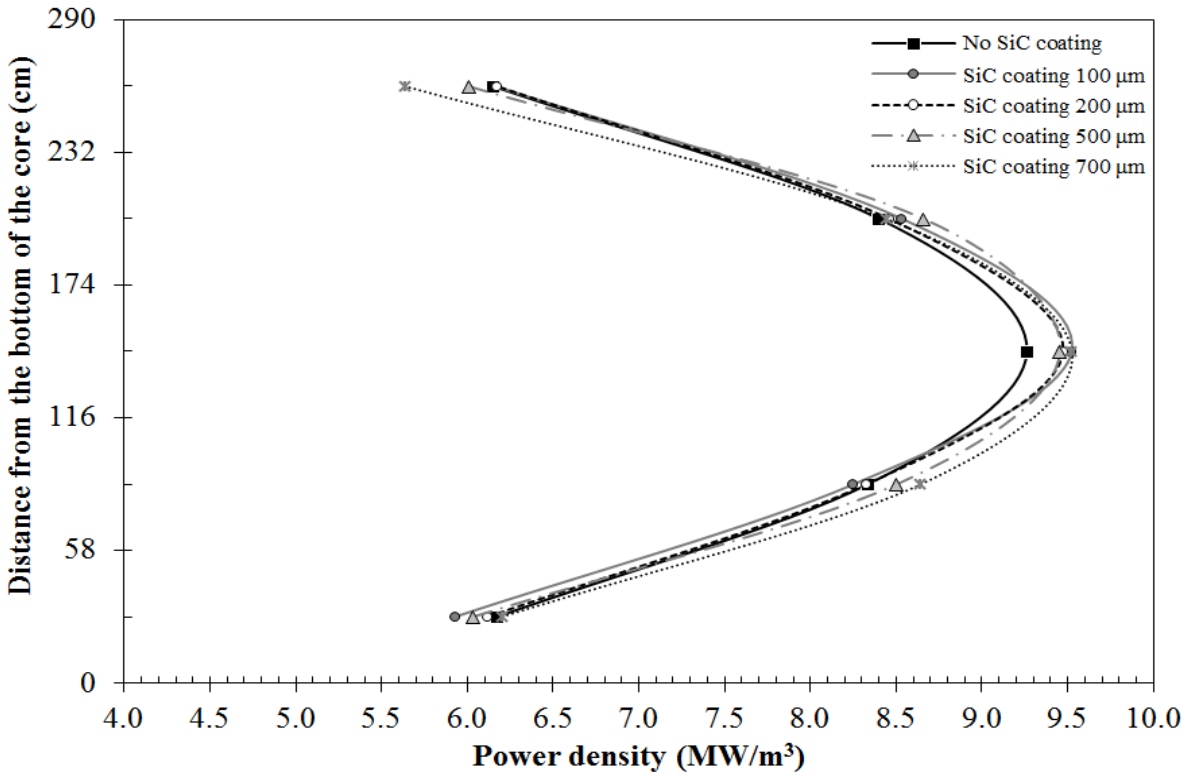

Figure 5 The axial power density distribution on the fuel rods at the peak power position during the beginning of the reactor cycle

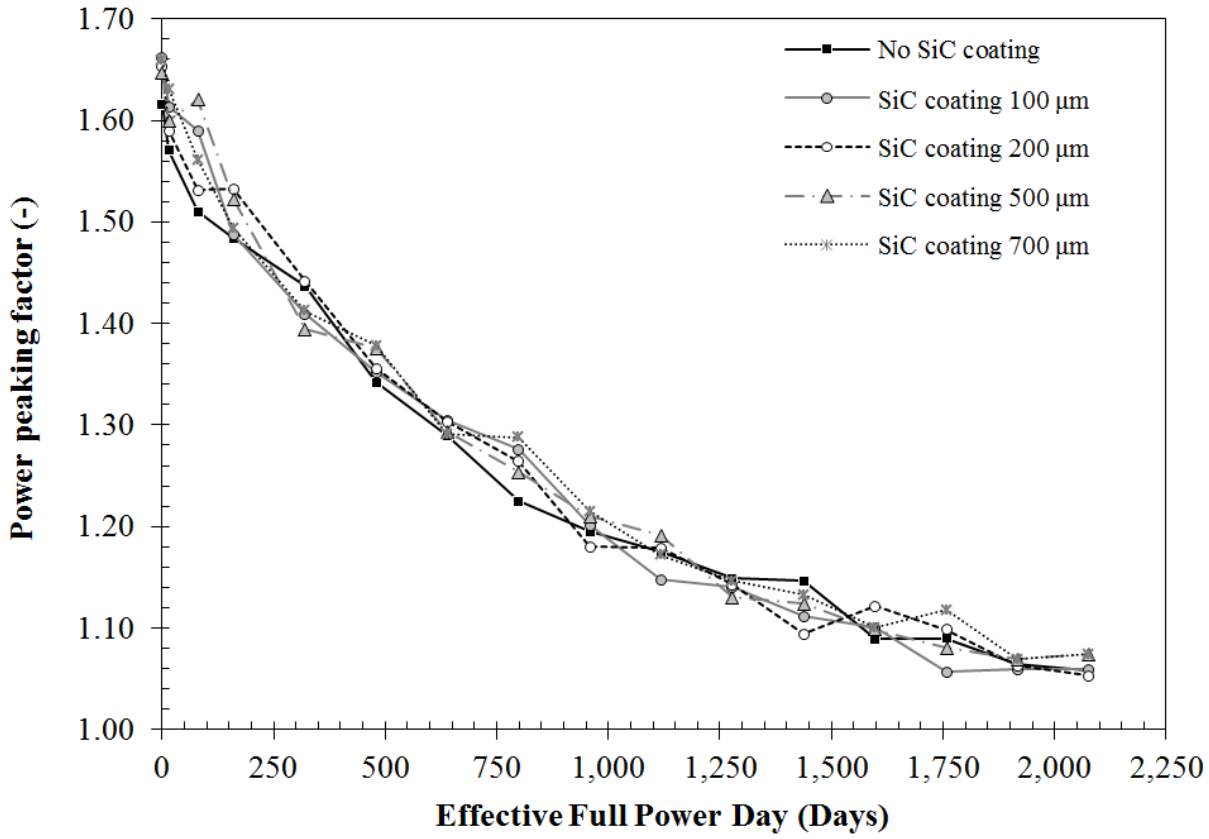

Figure 6 Power peaking factor of an HTGR during core life

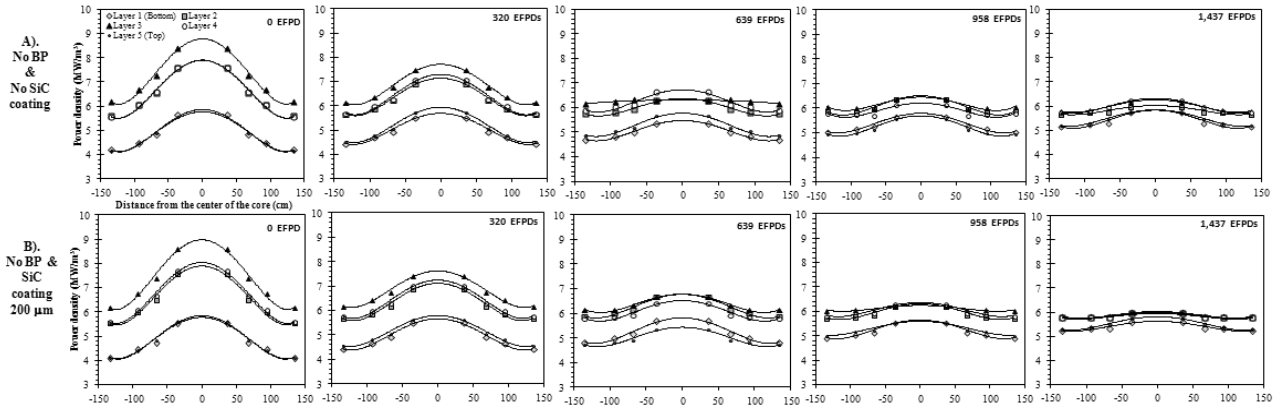

Figure 7 History of the radial power density distribution for 5-fuel block layers at the reactor operation of 0, 320, 639, 958 and 1,437 EFPDs for a conventional reactor and a reactor with a SiC coating layer of 200 μm coupled with no insertion of burnable poison

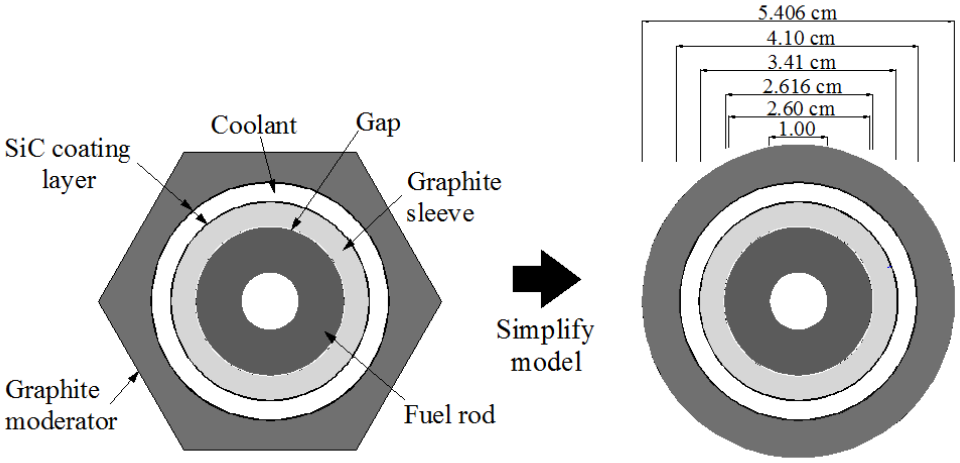

Figure 8 Cross-section view of single sub-channel model geometry

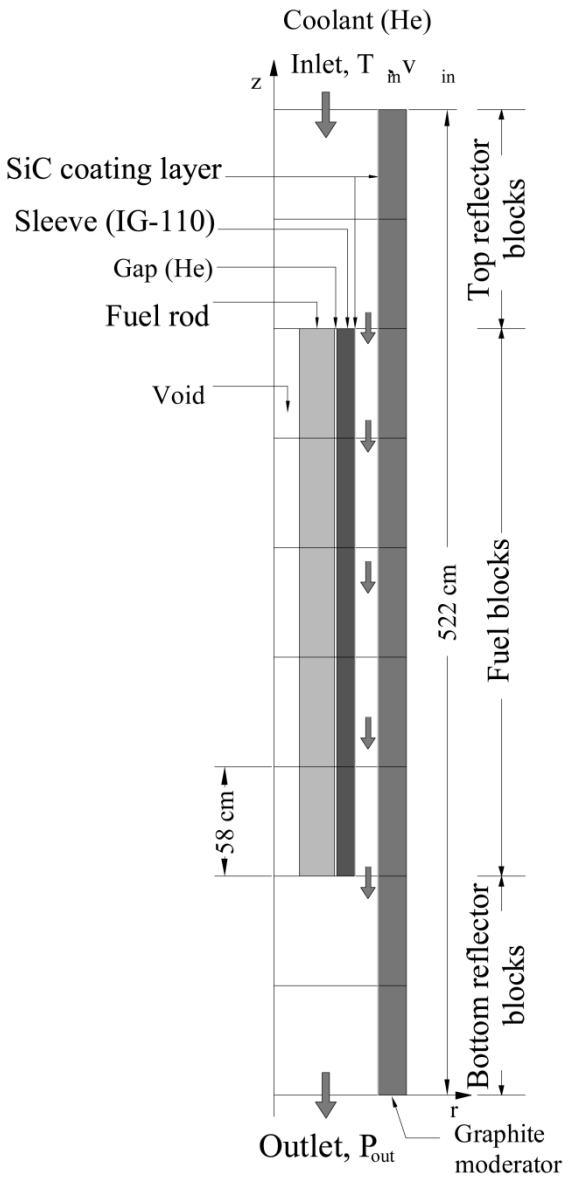

Figure 9 Geometry of sub-channel analysis for the whole length of the reactor

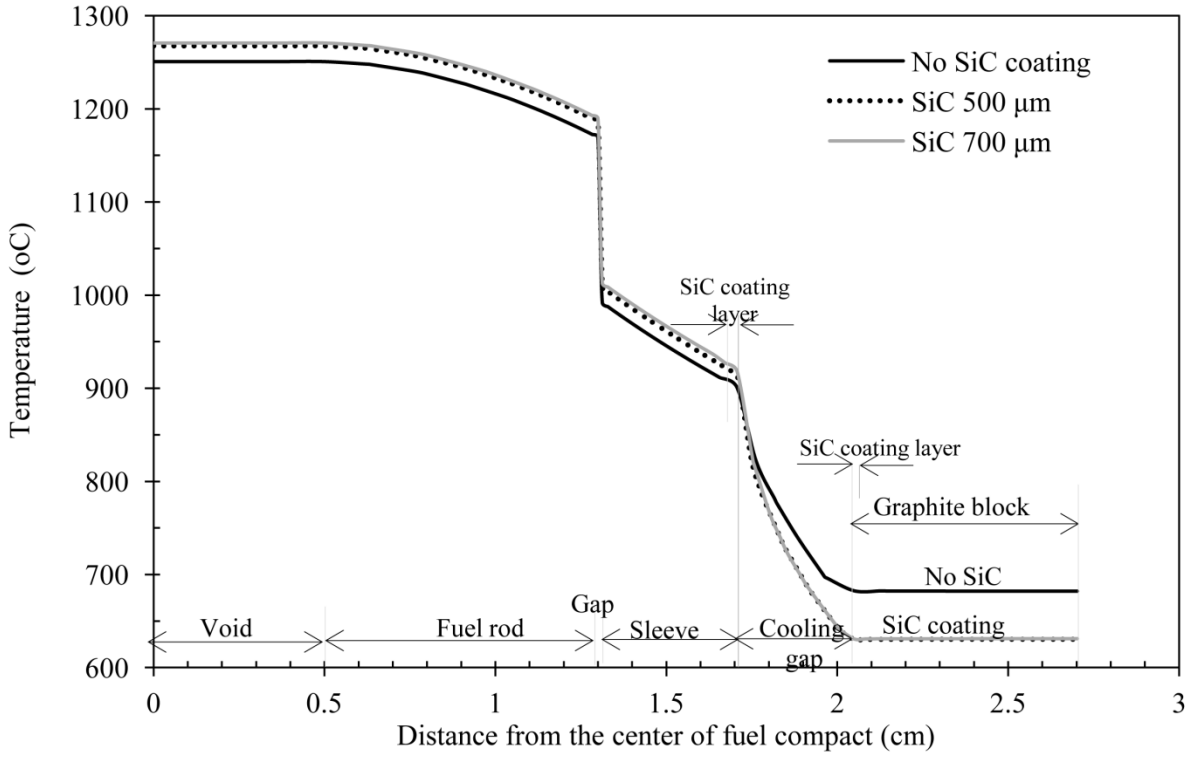

Figure 10 The temperature distribution in the radial direction at the middle of the core

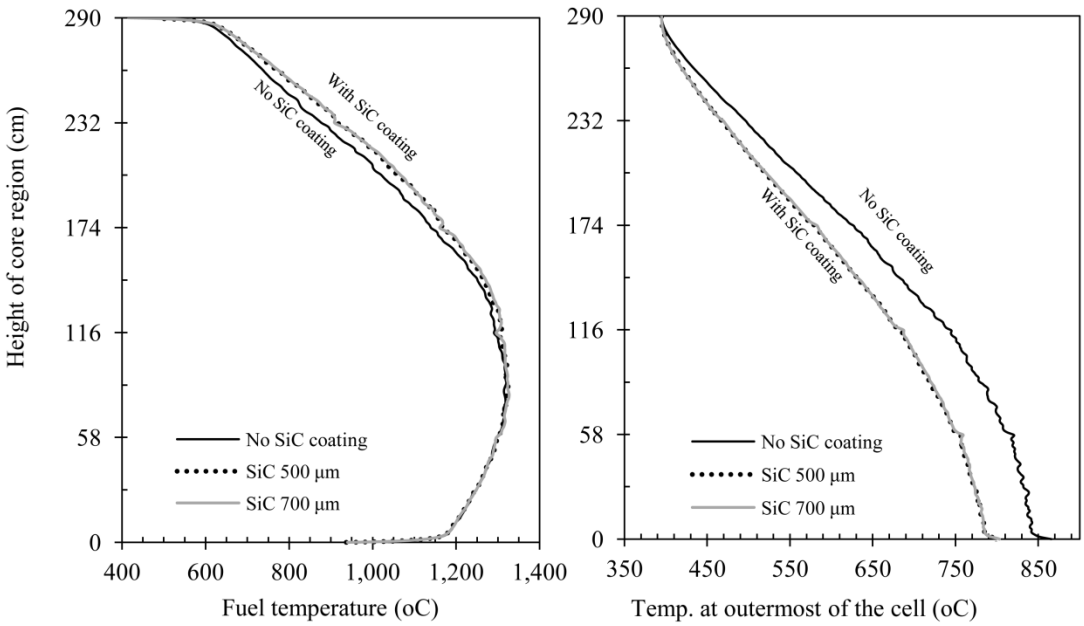

Figure 11 The temperature distribution in the axial direction